Halide-Stabilizing Residues of Haloalkane Dehalogenases Studied by Quantum Mechanic Calculations and Site-Directed Mutagenesis†

Michal Boháč,‡ Yuji Nagata,§ Zbyněk Prokop,‡ Martin Prokop,‡ Marta Monincová,‡ Masataka Tsuda,§ Jaroslav Koča,‡ and Jiří Damborský*,‡

National Centre for Biomolecular Research, Masaryk University, Kotlarska 2, 611 37 Brno, Czech Republic, and Graduate School of Life Sciences, Tohoku University, Katahira, Sendai 980-8577, Japan

Received July 10, 2002; Revised Manuscript Received October 4, 2002

ABSTRACT: Haloalkane dehalogenases catalyze cleavage of the carbon−halogen bond in halogenated aliphatic compounds, resulting in the formation of an alcohol, a halide, and a proton as the reaction products. Three structural features of haloalkane dehalogenases are essential for their catalytic performance: (i) a catalytic triad, (ii) an oxyanion hole, and (iii) the halide-stabilizing residues. Halide-stabilizing residues are not structurally conserved among different haloalkane dehalogenases. The level of stabilization of the transition state structure of S_N2 reaction and halide ion provided by each of the active site residues in the enzymes DhlA, LinB, and DhaA was quantified by quantum mechanic calculations. The residues that significantly stabilize the halide ion were assigned as the primary (essential) or the secondary (less important) halide-stabilizing residues. Site-directed mutagenesis was conducted with LinB enzyme to confirm location of its primary halide-stabilizing residues. Asn38Asp, Asn38Glu, Asn38Phe, Asn38Gln, Trp109Leu, Phe151Leu, Phe151Trp, Phe151Tyr, and Phe169Leu mutants of LinB were constructed, purified, and kinetically characterized. The following active site residues were classified as the primary halide-stabilizing residues: Trp125 and Trp175 of DhlA; Asn38 and Trp109 of LinB; and Asn41 and Trp107 of DhaA. All these residues make a hydrogen bond with the halide ion released from the substrate molecule, and their substitution results in enzymes with significantly modified catalytic properties. The following active site residues were classified as the secondary halide-stabilizing residues: Phe172, Pro223, and Val226 of DhlA; Trp207, Pro208, and Ile211 of LinB; and Phe205, Pro206, and Ile209 of DhaA. The differences in the halide stabilizing residues of three haloalkane dehalogenases are discussed in the light of molecular adaptation of these enzymes to their substrates.

Haloalkane dehalogenases are bacterial enzymes that catalyze hydrolytic dehalogenation of a broad range of halogenated compounds. Crystallographic studies provided structures for three different haloalkane dehalogenases: DhlA[1] from *Xanthobacter autotrophicus* GJ10 (*1*), DhaA from *Rhodococcus* sp. (*2*), and LinB from *Sphingomonas paucimobilis* UT26 (*3*). The active site of haloalkane dehalogenases is located between two domains. The main domain is formed by an eight-stranded β-sheet surrounded by α-helices and shares structural homology with α/β-hydrolases (*4*, *5*). The cap domain is composed of five α-helices and shares structural homology with uteroglobin (*6*).

Haloalkane dehalogenases use a three-step dehalogenation mechanism for cleavage of the carbon−halogen bond and formation of an alcohol, a halide, and a proton as the reaction products (Figure 1). The carbon atom attached to the leaving halogen is attacked by a nucleophile in a nucleophilic substitution reaction (S_N2), yielding an alkyl−enzyme intermediate. The released halide is stabilized by the residues of the enzyme active site. The alkyl−enzyme intermediate is hydrolyzed in a nucleophilic addition reaction (Ad_N), yielding a tetrahedral intermediate that further undergoes elimination reaction (E). Three structural features of haloalkane dehalogenases were recognized as essential for their catalytic performance: (i) a catalytic triad, (ii) an oxyanion hole, and (iii) the halide-stabilizing residues (*7*, *8*).

The catalytic triad composed of nucleophile, base, and acid is present in all three structurally characterized haloalkane dehalogenases. The essential role of the catalytic triad was revealed by crystallographic (*2*, *3*, *7*) and site-directed mutagenesis studies (*9*−*11*). Aspartic acid serves as a nucleophile, attacking the substrate molecule, and is located in a very sharp turn called the nucleophile elbow. Histidine serves as a base, abstracting the hydrogen from the hydrolytic water. The catalytic acid (Asp in DhlA; Glu in LinB and

† Financial support from the Czech Ministry of Education (Grants No. J07/98:143100005 and ME276) is acknowledged.

* To whom correspondence should be addressed. FAX: +420-5-41129506. E-mail: jiri@chemi.muni.cz.

‡ Masaryk University.

§ Tohoku University.

[1] Abbreviations: DhlA, haloalkane dehalogenase from *Xanthobacter autotrophicus* GJ10; DhaA, haloalkane dehalogenase from *Rhodococcus erythropolis* strains Y2, m15-3, HA1, GJ70, NCIMB13064, and TB2; LinB, haloalkane dehalogenase from *Sphingomonas paucimobilis* UT26; CBT, 1-chlorobutane; $\Delta E_{elst(TS-ES)}$, difference in electrostatic interaction energy between an amino acid residue and halogen in transition state and enzyme−substrate structures; $\Delta E_{elst(EP-ES)}$, difference in electrostatic interaction energy between an amino acid residue and halogen/halide in enzyme−product and enzyme−substrate structures; ES, enzyme−substrate; TS, transition state; EP, enzyme−product; E^a, activation energy; ΔH, reaction enthalpy; k_{cat}, catalytic constant.

10.1021/bi026427v CCC: $22.00
Published on Web 11/07/2002

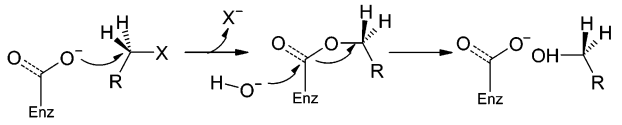

FIGURE 1: Reaction mechanism of haloalkane dehalogenases. Reaction is initiated by the attack of nucleophile on the substrate molecule, leading to the cleavage of carbon−halogen bond, halide release, and formation of the alkyl−enzyme intermediate. Alkyl−enzyme intermediate is hydrolyzed by activated water molecule yielding the primary alcohol.

DhaA) is hydrogen bonded to histidine, keeps its proper orientation, and increases the basicity of nitrogen in the imidazole ring.

Another catalytically important structural feature that is conserved in all three haloalkane dehalogenases (*8*) as well as in all α/β-hydrolases (*4*) is the oxyanion hole. The oxyanion hole is formed by two backbone nitrogen atoms. Amidic NH groups from tryptophan next to the nucleophile and from another residue located after strand β3 (Glu56 in DhlA, Asn38 in LinB, and Asn41 in DhaA) are hydrogen bonded to $O_{\delta 2}$ of the nucleophile, leading to an increase in the nucleophility of $O_{\delta 1}$ and stabilizing the negatively charged transition state that occurs during hydrolysis.

Unlike residues of the catalytic triad and the oxyanion hole, the halide-stabilizing residues are not present on equivalent positions in different haloalkane dehalogenases (*8*). Trp125 and Trp175 were identified as essential for stabilization of halide ion in DhlA by crystallographic and fluorescence study (*12*), site-directed mutagenesis (*13*−*15*) and quantum-mechanic calculations (*16*). Trp125 of DhlA is conserved also in LinB (Trp109) and DhaA (Trp107), while Trp175 is not conserved due to different architecture of the cap domain.

The objectives of this study were (i) to identify halide-stabilizing residues in LinB and DhaA enzymes and (ii) to compare the efficiency of stabilization in different haloalkane dehalogenases. Comparison of the halide-stabilizing residues in different enzymes is important for explaining their molecular evolution and for the proposal of mutations leading to enzymes with enhanced activity.

MATERIALS AND METHODS

Preparation of Active Site Models. Crystal structures of haloalkane dehalogenases from Protein Databank served as the input geometries for quantum mechanic calculations: 1EDE for DhlA (*17*), 1CV2 for LinB (*3*), and 1CQW for DhaA (*2*). All ions and water molecules except catalytic water were removed from the protein structures, and substrate 1-chlorobutane (CBT) was docked in protein active site using the program AUTODOCK 3.0 (*18*) and previously optimized parameters (*19*). The program WHATIF 5.0 (*20*) was used for adding the polar hydrogen atoms on protein structures. Catalytic histidines were singly protonated on N_{δ} in accordance with their catalytic function. Important active site residues for quantum-mechanic calculations were selected by structural and sequential comparisons. Each active site model consisted of 21 amino acids, the catalytic water, and the molecule of substrate. The model of DhlA consisted of Glu56, Asp124, Trp125, Phe128, Phe164, Pro168, Asp170, Phe172, Trp175, Leu179, Val180, Phe190, Trp194, Phe222, Pro223, Val226, Asp260, Leu262, Leu263, His289, and Phe290 (Figure 2A) with total charge −4. The model of LinB

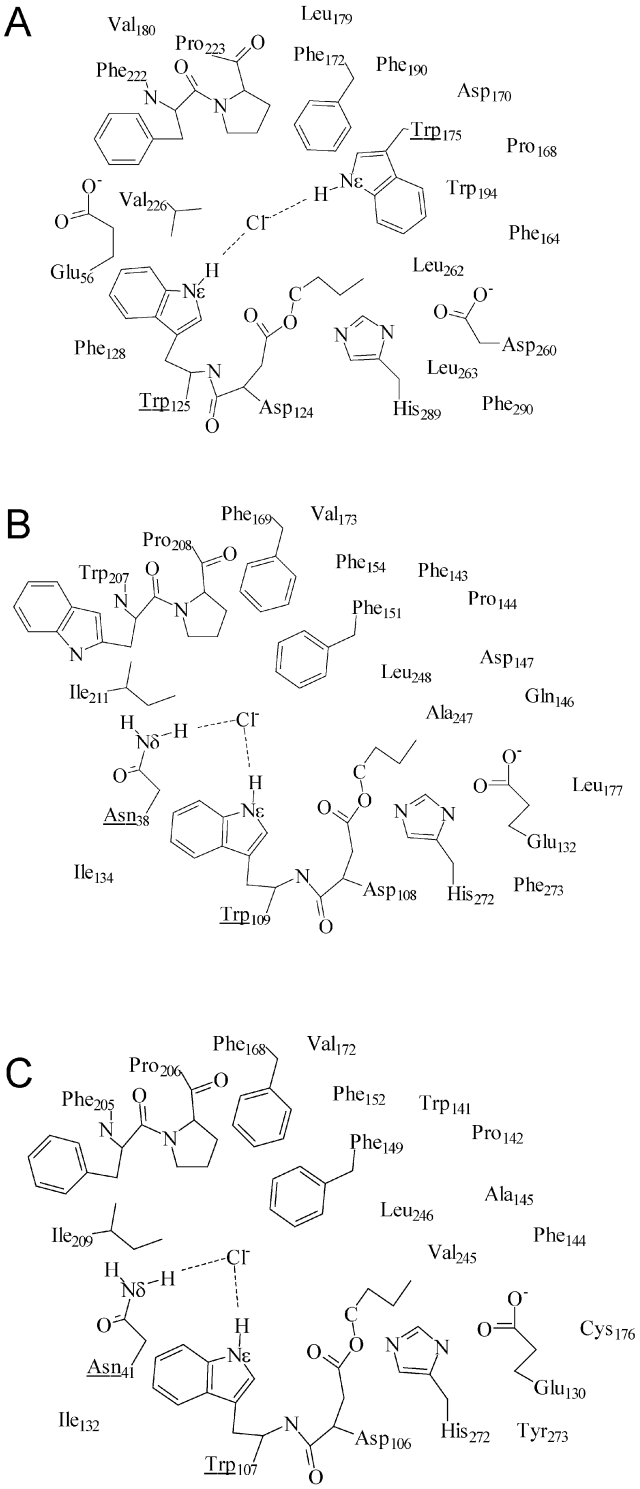

FIGURE 2: Schemes of the active sites of DhlA (A), LinB (B), and DhaA (C) composed of 21 amino acid residues used for modeling of enzymatic dehalogenation reaction. The enzymes are drawn in the state of alkyl−enzyme intermediate with bound chloride anion. Side chains of selected amino acid residues are not displayed for clarity. The residues providing hydrogen bonds to the chloride anion are underlined.

consisted of Asn38, Asp108, Trp109, Glu132, Ile134, Phe143, Pro144, Gln146, Asp147, Phe151, Phe154, Phe169, Val173, Leu177, Trp207, Pro208, Ile211, Ala247, Leu248, His272, and Phe273 (Figure 2B) with total charge −3. The model of DhaA consisted of Asn41, Asp106, Trp107, Glu130, Ile132, Trp141, Pro142, Phe144, Ala145, Phe149,

Phe152, Phe168, Val172, Cys176, Phe205, Pro206, Ile209, Val245, Leu246, His272, and Tyr273 (Figure 2C) with a total charge −2. Single-point mutants of LinB were constructed by the method of satisfaction of spatial restrains implemented in the program MODELLER 6.0a (*21*) using previously optimized parameters (*22*).

Modeling of Enzymatic Dehalogenation Reaction. The program MOPAC version 2000 (*23*) with the novel algorithm MOZYME (*24*) and the external subroutine DRIVER (*25*) was used for mapping of the reaction pathway. Semiempirical level of theory enabled inclusion of all first shell and many second shell residues into the calculation. Applicability of semiempirical methods for modeling of S_N2 dehalogenation reactions has been confirmed in previous studies (*16*, *22*, *26*). S_N2 reaction step was modeled by shortening the distance between the O_δ of the nucleophile and C_1 carbon of CBT attached to the chlorine atom. The distance was shortened by 0.05 Å with each driving step, and the system was fully optimized except the driven coordinate, heavy atoms of the protein backbone, and the hydrolytic water. All calculations were carried out using AM1 Hamiltonian with Mulliken population analysis for charge distribution and BFGS geometry optimization algorithm. The following optional keywords were used to control the calculation: GEO-OK, MMOK, NOINTER, NOXYZ, and CHARGE. Data analysis was performed using the program TRITON 2.0b (*27*, *28*). The activation energy (E^a) of the reaction was approximated as the difference between the heat of formation of the enzyme−substrate (ES) and the transition state (TS) structures, while the change of enthalpy (ΔH) was calculated as the difference between heat of formation of the ES and enzyme−product (EP) structures. The electrostatic interaction energies (E_{elst}) were calculated as the sum of all atom−atom interaction energies between each amino acid and chlorine atom of CBT (released chloride ion respectively), according to Coulomb law using the geometries and partial charges obtained from MOPAC calculations.

Modeling of Halide Stabilization. Total interaction energies between the halide ion and individual active site residues and their pairs (Trp175 and Trp125...Trp175 pair of DhlA; Tyr175 and Trp125...Tyr175 pair of Trp175Tyr mutant of DhlA; Asn38 and Asn38...Trp109 pair of LinB) were calculated at semiempirical and ab initio level of theory. Starting geometries were taken from the crystal structures with bound halide ion at the highest available resolution: 2DHD, the structure of DhlA with covalently bound chloroethyl, resolution 2.0 Å (*7*); 1B6G, the high-resolution structure of DhlA, resolution 1.2 Å (*29*); 1BEE, the structure of Trp175Tyr mutant of DhlA, resolution 2.6 Å (*14*), and the high-resolution structure of LinB, resolution 0.9 Å (Oakley et al., unpublished results). Program MOPAC2000 and method AM1 were used for semiempirical calculations. Program Gaussian98 (*30*) and methods B3LYP and MP2 with 6-31++G** basis set were used for ab initio calculations.

Construction and Purification of Mutant Proteins. Mutagenesis of haloalkane dehalogenase LinB was performed using the LA PCR in vitro mutagenesis kit (TaKaRa Shuzo Co., Kyoto, Japan) according to the provided protocol, except for using Pyrobest DNA polymerase (TaKaRa), whose fidelity is very high. All of the nucleotide sequences of mutants were confirmed by the dideoxy-chain termination method with an automated DNA sequencer ABI PRISM 310 (Applied Biosystems, Foster City). The oligonucleotides used are as follows: Asn38Asp (5′-CAG CAC GGC GAT CCG ACG-3′), Asn38Glu (5′-CAG CAC GGC GAG CCG ACG TCG-3′), Asn38Phe (5′-CAG CAC GGC TTC CCG ACG TCG-3′), Asn38Gln (5′-CAG CAC GGC CAG CCG ACG TCG-3′), Phe151Leu (5′-GGC CTG CAA CAG ATC GCG-3′), Phe151Tyr (5′-GGC CTG ATA CAG ATC GCG-3′), and Phe169Leu (5′-TTG TTC GAC CAA AAC ATT GTC-3′). The oligonucleotides used for the construction of Trp109Leu and Phe151Trp mutants were published earlier (*31*). Plasmids for overexpression of mutant proteins in *E. coli* were constructed from pAQN. *linB* mutants were transcribed by the *tac* promoter (P*tac*) under the control of *lacI*^{q} in these plasmids. *E. coli* JM109 containing constructed plasmids were cultured in 2 L of Luria broth at 37 °C. The induction of the enzyme expression was initiated by the addition of isopropyl-β-D-thiogalactopyranoside to a final concentration of 0.5 mM, when the culture reached an optical density of 0.6 at 600 nm. The cells were harvested and disrupted by sonication using a Sonopuls GM70 (Bandelin, Berlin, Germany). The supernatant was used after centrifugation at 100 000 × *g* for 1 h. The crude extract was further purified on a Ni−NTA Sepharose column (QIAGEN, Hilden, Germany). The His-tagged LinB (*31*) was bound to the resin in the equilibrating buffer (20 mM potassium phosphate buffer [pH 7.5] containing 0.5 M sodium chloride and 10 mM imidazole). Unbound and weakly bound proteins were washed out by the buffer containing 45 mM imidazole. The His-tagged enzyme was then eluted by the buffer containing 250 mM imidazole. The active fractions were pooled, dialyzed against a 50 mM potassium phosphate buffer [pH 7.5] overnight, and stored in a 50 mM potassium phosphate buffer [pH 7.5] containing 10% glycerol and 1 mM 2-mercaptoethanol.

Kinetic Characterization of Mutant Proteins. Catalytic activity of wild-type LinB and its mutants was assessed by determination of the substrate and product concentrations using a gas chromatograph (Trace GC 2000, ThermoQuest) equipped with the flame ionization detector and the capillary column DB−FFAP 30m × 0.25 mm × 0.25 μm (J&W Scientific, Folsom). Dehalogenation was performed in 25 mL Reacti-Flasks closed by Mininert Valves in a shaking water-bath at 37 °C. The reaction mixture consisted of enzyme preparation (4 mg/L) and varied concentrations of the substrate CBT (0.1−6.4 mM). The reaction was stopped by addition of methanol at three different times. The data were measured in triplicates, and the steady-state catalytic constant (k_{cat}) was calculated using the computer program EZ-Fit version 1.1 (author: F. W. Perrella).

RESULTS

Identification of Halide-Stabilizing Residues by Quantum Mechanic Calculations. Carbon−halogen bond cleavage was modeled in the active sites of DhlA, LinB, and DhaA enzymes using semiempirical quantum mechanic calculations. This theory enabled inclusion of all residues essential for proper modeling of S_N2 dehalogenation reaction into single calculation and identification of residues involved in halogen/halide stabilization. Calculated activation barriers of S_N2 reactions in DhlA, LinB, and DhaA were 21, 19, and 20 kcal/mol, respectively. Calculated enthalpies were −16,

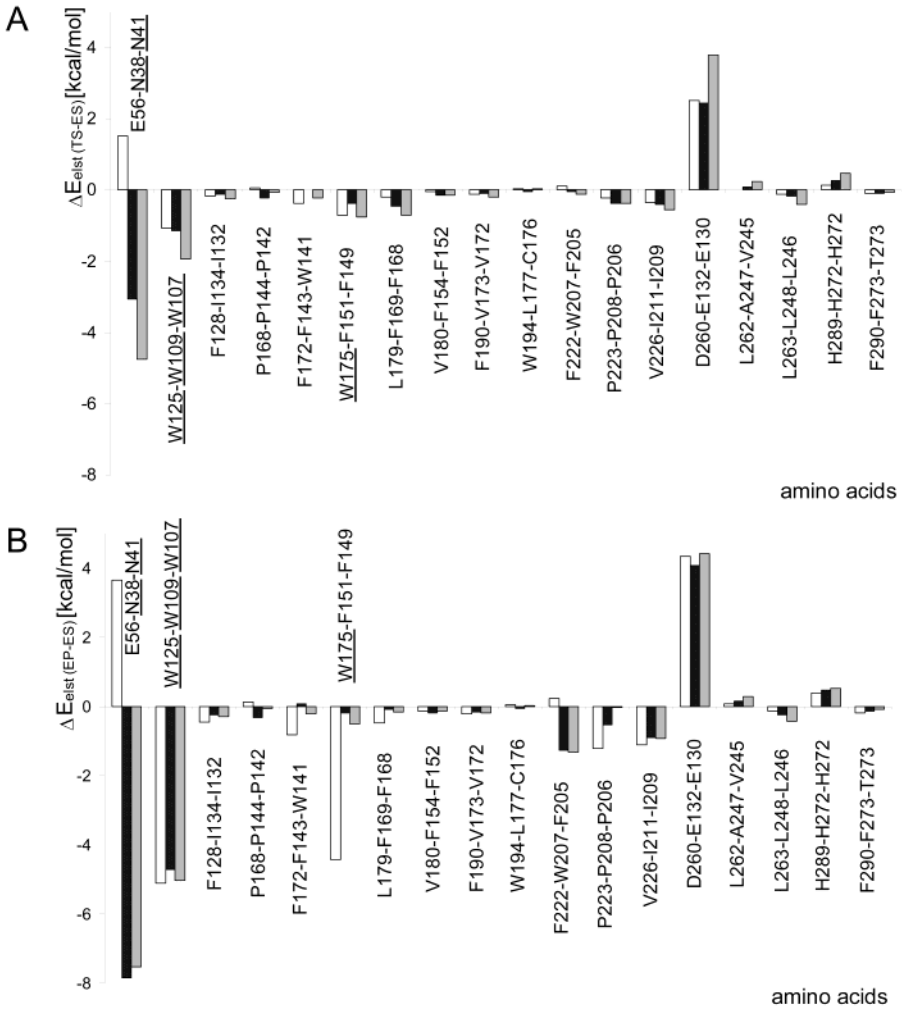

FIGURE 3: Electrostatic interaction energies for the selected equivalent amino acid residues of DhlA (white), LinB (black), and DhaA (grey). The energy differences between a transition state (TS) and an enzyme−substrate (ES) are on the panel A, while the energy differences between an enzyme−product (EP) and an enzyme−substrate (ES) are on panel B. The residues providing hydrogen bonds to the chloride anion are underlined.

−13, and −15 kcal/mol, respectively. These values suggest that the reaction course is similar for all three studied enzymes. The differences in the energies among enzymes are within an error of calculation conducted with structures prepared by a molecular docking. Estimated changes in electrostatic interaction energies between halogen/halide and each of the active site residues during the reaction course were used to obtain quantitative information about the role of each amino acid residue for stabilization of transition state and products of S_N2 reaction. Electrostatic interactions were suggested to play key role in stabilization of halide ions by haloalkane dehalogenases in both experimental (*12*−*14*, *32*−*34*) and theoretical studies (*16*, *22*, *26*, *35*−*39*). $\Delta E_{elst(TS-ES)}$ quantifies the stabilization of the transition state, while $\Delta E_{elst(EP-ES)}$ quantifies stabilization of the product, on a per-residue basis. Figure 3 shows $\Delta E_{elst(TS-ES)}$ (panel A) and $\Delta E_{elst(EP-ES)}$ (panel B) values for equivalent amino acid residues of DhlA, LinB, and DhaA. The residues showing significant changes in electrostatic energies, except the nucleophile, are discussed in the following text. The nucleophile is not discussed because its side-chain is covalently modified during the reaction.

Active Site Residues Glu56-Asn38-Asn41. Glu56 of DhlA makes very different electrostatic interactions with the halogen moiety compared to Asn38 of LinB and Asn41 of DhaA. Repulsion of about +1.5 kcal/mol in TS and +3.7 kcal/mol in EP is due to its negative charge, which makes unfavorable interactions of this residue with the chloride anion. The distance between C_δ of Glu56 and Cl^- is about 5.5 Å (Table 1). This residue is rotated out of the active site. Equivalent residues in LinB (Asn38) and DhaA (Asn41) show significant attraction with $\Delta E_{elst(TS-ES)} = -3.7$ and −4.8 kcal/mol and $\Delta E_{elst(EP-ES)} = -7.9$ and −7.5 kcal/mol. Both Asn38 and Asn41 are pointing toward the active site cavity. Higher stabilization of Cl^- in EP is both due to enlarged partial negative charge on the halide ion and shorter distance between $N_\delta H$ and Cl^- during the reaction (Table 1). The distance shortened from 2.6 Å in ES down to 2.0 Å in EP of Asn38 and from 2.6 Å in ES to 2.0 Å in EP of Asn41 due to repositioning of their side chains. This is in part an artifact of the calculation conducted with incomplete protein structure. Inclusion of additional second shell residues was not however computationally feasible. Nevertheless, distance, orientation and interaction energies all indicate the presence of a hydrogen-bond between Asn-$N_\delta H$ and Cl^-.

Trp125−*Trp109*−*Trp107.* A tryptophan residue located next to the nucleophile is strictly conserved in all currently known haloalkane dehalogenases (*40*). This residue holds the substrate molecule bound to the active site in the proper orientation for nucleophilic attack. Furthermore, it plays a

Table 1: Distances (in Å) between Selected Residues and Halogen/Halide in Modeled Enzyme−Substrate (ES), Transition State (TS), and Enzyme−Product (EP) Structures

DhlA	ES	TS	EP	LinB	ES	TS	EP	DhaA	ES	TS	EP
Glu56−Cδ	5.4	6.0	5.6	Asn38−NδH	2.6	2.6	2.0	Asn41−NδH	2.6	2.5	2.0
Trp125−NϵH	2.8	3.3	2.0	Trp109−NϵH	3.7	3.7	2.3	Trp107−NϵH	3.1	3.4	2.1
Phe172−CϵH	3.1	2.8	2.8	Phe143−CζH	5.4	5.2	6.4	Trp141−CηH	5.8	5.5	6.2
Trp175−NϵH	2.7	2.6	1.9	Phe151−CϵH	2.8	2.7	3.6	Phe149−CϵH	3.5	3.1	3.8
Leu179−CδH	5.0	5.2	5.1	Phe169−CζH	3.0	2.8	3.8	Phe168−CζH	3.5	2.9	3.9
Phe222−CβH	4.8	5.2	4.3	Trp207−CβH	3.6	3.8	2.5	Phe205−CβH	3.1	3.6	2.5
Pro223−CαH	2.9	3.5	2.6	Pro208−CαH	3.2	3.3	2.9	Pro206−CαH	3.2	3.3	3.1
Val226−CγH	3.0	3.0	2.8	Ile211−CδH	2.8	2.7	2.9	Ile209−CδH	2.8	2.7	2.9
Asp260−Cγ	10.6	9.9	10.9	Glu132−Cδ	11.5	11.2	12.3	Glu130−Cδ	11.5	11.1	11.7
His289−Nϵ	7.2	6.4	7.0	His272−Nϵ	6.5	6.3	7.3	His272−Nϵ	6.2	6.3	6.8

very important role for stabilization of TS ($\Delta E_{elst(TS-ES)}$ −1.1, −1.1, and −1.9 kcal/mol) and EP ($\Delta E_{elst(EP-ES)}$ −5.1, −4.7 and −5.0 kcal/mol). Distances between N$_\epsilon$H of Trp and Cl$^-$ were shortened to 2.0, 2.3, or 2.1 Å in EP (Table 1). Geometry and attractive interactions indicate the presence of a hydrogen bond between the chloride ion and tryptophan in all three enzymes.

Phe172−Phe143−Trp141. Phe172 differs from Phe143 and Trp141 in its efficiency to stabilize Cl$^-$ having $\Delta E_{elst(EP-ES)}$ = −0.8 kcal/mol compared to +0.1 and −0.2 kcal/mol. Phe172 appears to be important for stabilizing the halide ion (but not TS) in DhlA (*16*, *22*), while equivalent residues in LinB and DhaA do not provide such stabilization. Phe172 in EP is located much closer to Cl$^-$ than Phe143 or Trp141 (2.8 Å vs 6.4 and 6.2 Å; Table 1).

Trp175−Phe151−Phe149. Trp175 is the second most important residue for stabilization of halide ion in DhlA but has no analogue in LinB and DhaA. Stabilization of TS is similar in all three proteins with $\Delta E_{elst(TS-ES)}$ = −0.7, −0.4, and −0.8 kcal/mol. However, a large increase in electrostatic interaction between Trp175 and halide ion upon its release from CBT ($\Delta E_{elst(EP-ES)}$ −4.4 kcal/mol) is not observed with Phe151 and Phe149. Increased stabilization is due to repositioning of Trp175 (Table 1) that was noted in former studies (*16*). In contrast, the stabilizing role of Phe151 and Phe149 decreases during formation of the chloride anion ($\Delta E_{elst(EP-ES)}$ −0.2 and −0.5 kcal/mol), which is due to the strong attraction of Cl$^-$ by Asn38 and Asn41, respectively. Repositioning of Cl$^-$ in LinB and DhaA is apparent from the change in distances: from 2.8 Å (ES) through 2.7 Å (TS) to 3.6 Å (EP) for Phe151 and from 3.5 Å (ES) through 3.1 Å (TS) to 3.8 Å (EP) for Phe149 (Table 1).

Leu179−Phe169−Phe168. Examination of $\Delta E_{elst(TS-ES)}$ values for Phe169 and Phe168 reveals that these residues act similarly as Phe151 and Phe149 discussed in the previous paragraph. Also, the distances between these residues and the halogen atom are similar (Table 1). The distance between Phe169 and chlorine/chloride changed from 3.0 Å (ES) through 2.8 Å (TS) to 3.8 Å (EP), and the distance between Phe168 and chlorine/chloride changed from 3.5 Å (ES) through 2.9 Å (TS) to 3.9 Å (EP). These residues serve mainly for the stabilization of TS. After formation of the negative charge on Cl$^-$ and its strong attraction by Asn38 and Asn41, respectively, the distance rises, and halide stabilization by Phe169 and Phe168 is only marginal. Leu179 of DhlA is more than 5 Å from the chloride, and its $\Delta E_{elst(EP-ES)}$ is close to zero.

Phe222−Trp207−Phe205. These residues are close enough to interact with Cl$^-$ by weak interactions of hydrogens on C$_\beta$. The rest of the side chain is oriented out of the active site, and the stabilizing role of these residues is significantly independent of the residue type. Phe222 differs in $\Delta E_{elst(EP-ES)}$ from Trp207 and Phe205 (+0.3 vs −1.3 and −1.3 kcal/mol), which is probably due to the different position of Cl$^-$ in different dehalogenases (Table 1).

Pro223−Pro208−Pro206. Proline is another strictly conserved residue of haloalkane dehalogenases (*40*). It is in direct contact with the halogen atom of the substrate and halide ion released during the dehalogenation reaction. Significant difference in $\Delta E_{elst(EP-ES)}$, among the prolines of DhlA versus LinB and DhaA, is caused by different position of Cl$^-$ in EP. C$_\alpha$H in Pro223 is much closer to Cl$^-$ (2.6 Å) than C$_\alpha$H of Pro208 (2.9 Å) and Pro206 (3.1 Å).

Val226−Ile211−Ile209. Aliphatic residues Val226, Ile211, and Ile209 point toward the halogen/halide by their side chains. The distances between their nearest hydrogen and halogen/halide were changing only slightly during the reaction (always between 2.7 and 3.0 Å in all three enzymes) providing interactions $\Delta E_{elst(EP-ES)}$ −1.1, −0.9, and −0.9 kcal/mol.

Asp260−Glu132−Glu130. Second acids of the catalytic triad play a critical role during the catalytic cycle of the haloalkane dehalogenases. Although they are located far from chloride anion (Table 1), they show strong repulsion ($\Delta E_{elst(EP-ES)}$ +4.4, +4.1, and +4.4 kcal/mol) in all three enzymes. Substitution of the catalytic acid by an electroneutral residue, providing a more favorable interaction with the halide ion, is not possible for mechanistic reasons.

His289−His272−His272. Histidines are the members of the catalytic triad and are strictly conserved among all haloalkane dehalogenases (*40*). They show repulsion with chlorine/chloride but, like the above-discussed catalytic acid, cannot be modified for mechanistic reasons.

Validation of Primary Halide-Stabilizing Residues of LinB by Site-Directed Mutagenesis. Theoretical analysis of the electrostatic interaction energies revealed that the active site of DhlA contains two primary halide-stabilizing residues, Trp125 and Trp175, and three secondary halide-stabilizing residues: Phe172, Pro223, and Val226. One out of two key stabilizing residues of DhlA, tryptophan next to the nucleophile (Trp125), is also conserved in LinB (Trp109) and DhaA (Trp107), while the second tryptophan is not conserved and its role can be taken over either by one of the phenylalanines in equivalent position within the protein structure (Phe151 or Phe169 in LinB, Phe149 or Phe168 in DhaA) or by the asparagine showing high interaction energy in the quantum mechanic calculations (Asn38 in LinB, Asn41 in DhaA). Secondary halide-stabilizing residues in LinB are Trp207,

Table 2: Theoretical and Experimental Characteristics of LinB Proteins

protein	$\Delta\Delta E_{elst(TS-ES)}$[a] [kcal/mol]	$\Delta\Delta E_{elst(EP-ES)}$[a] [kcal/mol]	k_{cat} [s^{-1}]
wt	0	0	1.34
Asn38Asp	6.1	12.6	ND[b]
Asn38Glu	5.9	11.7	ND[b]
Asn38Phe	0.7	4.0	ND[b]
Asn38Gln	0.2	1.0	ND[b]
Trp109Leu	0.7	3.8	ND[b]
Phe151Leu	0.3	0.1	4.12
Phe151Trp	−0.2	−0.8	1.67
Phe151Tyr	0.2	0.2	1.73
Phe169Leu	0.2	−0.2	0.42

[a] Differences in electrostatic interaction energies between mutant and wild-type enzyme. [b] Activity not detectable.

Pro208, and Ile211, while analogous residues in DhaA are Phe205, Pro206, and Ile209. In silico and experimental site-directed mutagenesis of LinB was conducted to confirm the presence of primary halide-stabilizing residues in this protein. Substitutions in the primary residues are expected to result in the proteins with significantly changed activities. The following substitutions were introduced into LinB structure: Asn38Asp, Asn38Glu, Asn38Phe, Asn38Gln, Trp109Leu, Phe151Leu, Phe151Trp, Phe151Tyr, and Phe169Leu. The S_N2 reaction step was modeled for each mutant using the same approach as previously described for the wild-type enzymes. The values of $\Delta E_{elst(TS-ES)}$ and $\Delta E_{elst(EP-ES)}$ were calculated for each mutant and compared with values obtained for the wild-type enzyme. Interaction energies listed in Table 2 quantify the difference in halide stabilization between the mutant and wild-type enzymes; i.e., positive values of $\Delta\Delta E_{elst(TS-ES)}$ and $\Delta\Delta E_{elst(EP-ES)}$ indicate worse stabilization by mutant compared to the wild-type enzyme and vice versa. Each mutant was also constructed, purified, and kinetically characterized (Table 2).

Asn38Asp, Asn38Glu, Asn38Phe, and Asn38Gln. The mutants Asn38Asp and Asn38Glu showed lower stabilization of chlorine in TS than the wild-type enzyme by about 6 kcal/mol. Effect of mutation on chloride stabilization in EP was disfavored by about 12 kcal/mol. This very large change in the interaction energies is due to introduction of negative charge in the structure (note that Glu is present in the equivalent position in DhlA). No catalytic activity was measured for these mutants. Mutation Asn38Phe reduced stabilization of halogen in TS by 0.7 kcal/mol and stabilization of halide in EP by 4 kcal/mol. Reduction in stabilization is not so pronounced as that in previously discussed mutations Asn38Asp and Asn38Glu. Still, this mutant did not show any activity in the experiment. Substitution of Asn38 by structurally and physicochemically similar Gln in Asn35Gln mutant reduced stabilization of halogen in TS only by 0.2 kcal/mol and stabilization of halide in EP by 1 kcal/mol. Even this mutant however did not show any activity with CBT, suggesting that geometry of the halide-binding site must be preserved very precisely in LinB. Even extension of the side chain by a single carbon atom completely diminished activity of LinB confirming the essential role of Asn38 in the catalysis.

Trp109Leu. One single-point mutant in the position 109 of LinB was constructed providing a catalytically inactive protein. Modeling of the reaction showed that Trp109 is less important for the stabilization of halogen in TS ($\Delta\Delta E_{elst(TS-ES)}$ = 0.7 kcal/mol) than for the stabilization of halide in EP ($\Delta\Delta E_{elst(EP-ES)}$ = 3.8 kcal/mol). These results confirm the key role of Trp109 for halide stabilization and the catalysis.

Phe151Leu, Phe151Trp, and Phe151Tyr. Three different amino acids were introduced in position 151 of LinB. If Phe151 is a primary stabilizing residue, then inefficient halide stabilization and low activity would be expected for Phe151Leu mutant. Theoretical calculations however revealed that all three substituted residues provided sufficient stabilization ($\Delta\Delta E_{elst(TS-ES)}$ ranging from −0.2 to 0.3 kcal/mol and $\Delta\Delta E_{elst(EP-ES)}$ ranging from −0.8 to 0.2 kcal/mol), and kinetic analysis confirmed good activity for all three mutants. In fact, three mutants showed higher activity with CBT than the wild-type enzyme. Mutations apparently influenced not only S_N2 step but also other catalytic steps of LinB.

Phe169Leu. Mutation Phe169Leu did not affect stabilization ($\Delta\Delta E_{elst(TS-ES)}$ = 0.2 kcal/mol and $\Delta\Delta E_{elst(EP-ES)}$ −0.2 kcal/mol), showing the differences in interaction energies from wild-type enzyme within an error of calculation. Kinetic characterization of Phe169Leu mutant revealed lower, but significant, activity with CBT. It can be concluded that neither Phe151 nor Phe169 serves as the primary halide-stabilizing residues of LinB.

Estimation of Stabilization Efficiency of Primary Halide-Stabilizing Residues by Quantum Mechanic Calculations. Site-directed mutagenesis experiments confirmed that LinB and DhaA possess different primary halide-stabilizing residues than DhlA. Halogen/halide is stabilized by a Trp...Trp pair in DhlA but an Asn...Trp pair in LinB and DhaA. It can be expected that the efficiency of stabilization provided by the pair of primary residues will have significant impact on the catalytic performance of an enzyme by influencing the different steps of the catalytic cycle. Stabilization of the halide ion in crystal structures of haloalkane dehalogenases was studied by semiempirical and ab initio quantum mechanic calculations. Total interaction energies between the halide ion and amino acids serving as the primary halide-stabilizing residues, as well as their pairs, were calculated (Table 3). Absolute values of total interaction energy calculated using semiempirical and ab initio methods are not directly comparable, but the stabilization effects of different amino acid residues can be compared among methods. Input geometries were taken from the experimental structures, solved to high resolution when available, to ensure their high accuracy. Besides high-resolution structures of wild-type enzymes of DhlA and LinB in a complex with chloride ion, the alkyl enzyme intermediate of DhlA and Trp175Tyr mutant of DhlA were also included in the calculations (Table 3). Trends in stabilization among residues were the same irrespective of the method used for the calculation: (i) interaction energies of free enzyme−halide ion complex and alkyl−enzyme intermediate−halide ion complex are the same, (ii) stabilization efficiency of different amino acid residues is in the order Trp > Asn ≫ Tyr, and (iii) stabilization efficiency of the primary halide-stabilizing residues is in the order Trp...Trp > Trp...Asn ≫ Trp...Tyr. Experimentally derived K_d values for chloride ions follow the same trend: K_d for chloride and DhlA (*41*) is 75 mM (pH 8.2, 30 °C); K_d for chloride and LinB (Prokop et al., unpublished results) is 805 mM (pH 8.6, 37 °C); and K_d for

Table 3: Total Interaction Energies (in kcal/mol) between Primary Halide-Stabilizing Residues and Halide in X-Ray Structures

method/basis set	Trp[a]	Trp[b]	Tyr[c]	Asn[d]	Trp...Trp[a]	Trp...Trp[b]	Trp...Tyr[c]	Asn...Trp[d]
AM1	−22.8	−21.7	−4.8	−14.3	−35.7	−37.0	−19.3	−28.9
B3LYP/6-31++G**	−21.9	−21.5	−6.0	−17.9	−36.4	−37.4	−22.6	−33.8
MP2/6-31++G**	−25.8	−25.2	−8.3	−20.2	NA[e]	NA[e]	NA[e]	NA[e]

[a] Geometry from DhlA structure with covalently bound chloroethyl (PDB ID 2DHD). [b] Geometry from high-resolution structure of DhlA (PDB ID 1B6G). [c] Geometry from Trp175Tyr mutant structure of DhlA (PDB ID 1BEE). [d] Geometry from high-resolution structure of LinB (Oakley et al., unpublished). [e] Not applicable (system is too large).

chloride and Trp175Tyr DhlA (*14*) is >1000 mM (pH 8.2, 30 °C).

DISCUSSION

Practical application of haloalkane dehalogenases in environmental technologies (*42*) and chemical syntheses (*43*) is hindered by their low conversion rates with target chemicals. A number of mutagenesis studies have already been conducted with these enzymes, but obtained enhancements of the catalytic rates were on 1 order of magnitude at best (*19*, *33*, *44*, *45*). Even directed evolution experiments with good potential for broad exploitation of the sequence space have not been more successful so far (*46*, *47*). Pikkemat and Janssen (*47*) proposed that the difficulties with enhancement of the catalytic performance of DhlA may arise from the fact that the protein is trapped in its local evolutionary optimum. What is this "evolutionary optimum" in structural terms, and why is it so difficult to improve the catalytic performance of DhlA by modification of its structure? Pre-steady-state kinetic characterization of single-point mutants of DhlA revealed that enhancement of the rate for one catalytic step results in reduced rate for another step (*14*, *33*, *48*). In particular, formation of the enzyme−substrate complex, cleavage of the carbon−halogen bond and halide release seems to be kinetically inter-linked. This is understandable, considering that (i) good binding and high stabilization of the halogen atom in a substrate molecule is favorable for the process leading to the formation of a Michaelis complex, (ii) high stabilization of the developing charge on the halogen atom in TS of S_N2 is favorable for the reaction, but (iii) high stabilization of the halide ion in the enzyme active site after the reaction is unfavorable for the halide release. Three above-discussed catalytic steps are related also structurally because the same amino acid residues of the active site are involved in halogen/halide binding. Identification of these residues in three different haloalkane dehalogenases (Figure 4) and comparison of their stabilization efficiency are described here as part of our effort to improve catalytic performance of haloalkane dehalogenases by the rational approach.

Trp125 and Trp175 are well-known halide-stabilizing residues of DhlA based on previous experimental and theoretical studies (*12*−*16*). Their role for the transition state and halide stabilization is also clearly supported by the calculations presented in this report. The interaction energy between Trp175 and halogen moiety increases during the reaction course due to change in distance between the halide ion and the tryptophan. Repositioning of Trp175 during the dehalogenation reaction was noted in previous quantum mechanic calculations (*16*) and is supported by the flexibility of this residue in molecular dynamics simulations (*38*, *49*). Trp175 is positioned in a flexible region of DhlA (*49*) of recent evolutionary origin (*47*, *50*). Its high mobility could be part of molecular adaptation for destabilization of the enzyme−product complex during the halide release, which is the rate-limiting catalytic step of DhlA (*51*).

Glu56 is together with Asp124 and Asp260 the only charged residue in the active site of DhlA. While Asp124 and Asp260 are the members of the catalytic triad and as such must be present in the active site, the presence of Glu56 is somewhat surprising because it makes unfavorable repulsion with halogen/halide. We propose that Glu56 is another adaptation of DhlA for destabilization of enzyme−product complex. Although its side chain is pointing out of the active site, it was found to rotate occasionally into the active site cavity (*49*, *52*). Negative charge on Glu56 may serve as the additional force for expulsion of the halide from deeply buried active site cavity. The active site of DhlA must be small and buried for effective binding and desolvation of its natural substrate 1,2-dichloroethane (*8*, *53*).

Trp125 is conserved in all three dehalogenases, while Trp175 and Glu56 are not. The asparagine in the position structurally equivalent to Glu56 is taking the role of Trp175 in LinB and DhaA as predicted earlier by Newman et al. (*2*) and Marek et al. (*3*). This proposal was confirmed here by site-directed mutagenesis. Mutagenesis experiments also ruled out the possibility that the function of Trp175 is fulfilled by its structural equivalents Phe151 and Phe169 of LinB. We conclude that the Trp125...Trp175 pair in DhlA is functionally equivalent to the Asn38...Trp109 pair in LinB and the Asn41...Trp107 pair in DhaA (so-called primary halide-stabilizing residues; Figure 4). Both primary halide-stabilizing residues of LinB and DhaA are rigid (*49*), and the active sites of these enzymes do not contain any negatively charged residues except nucleophile and the catalytic acid, suggesting that destabilization of enzyme−product complex is not facilitated by the same mechanisms as in DhlA. Halide release in LinB and DhaA should be faster than in DhlA because (i) their active sites are more open to the solvent and (ii) stabilization of the halide ion by the Asn...Trp pair is weaker compared to that by the Trp...Trp pair. Recent pre-steady-state kinetic analysis of LinB confirmed that halide release is not a limiting step for the catalytic cycle of this enzyme (Prokop et al., unpublished).

There are additional residues in haloalkane dehalogenases with significant changes in electrostatic interactions during the reaction course. These residues do not make a hydrogen bond with the halide ion, they are not essential for catalysis and are therefore reported here as secondary halide-stabilizing residues: Phe172, Pro223, and Val226 in DhlA; Trp207, Pro208, and Ile211 in LinB; and Phe205, Pro206, and Ile209 in DhaA (Figure 4). Phe172 in DhlA has no obvious equivalent in DhaA and LinB. The role of Phe172 for catalysis of DhlA was extensively studied by site-directed

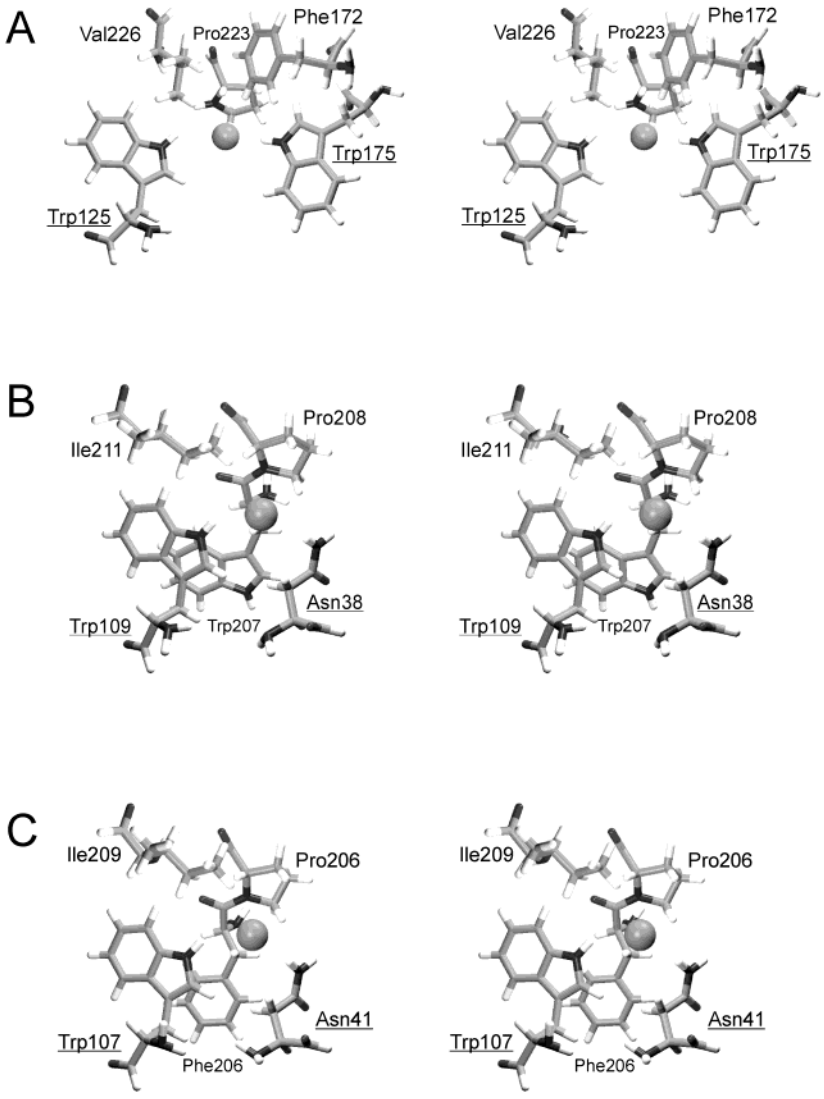

FIGURE 4: Stereoview of the halide-stabilizing residues of DhlA (A), LinB (B), and DhaA (C). The halide ions are shown as balls. The primary halide-stabilizing residues providing hydrogen bonds to the chloride anion are underlined.

mutagenesis, pre-steady-state kinetics and protein crystallography (*33*) as well as by quantum mechanics calculations (*22*) and quantitative structure−function relationship analysis (*54*). These studies clearly confirmed participation of this residue in stabilization of TS of the carbon−halogen bond cleavage and stabilization of halide ion. The mutant Phe172Trp showed reduced rate of S_N2 reaction, but enhanced halide release in experiment with 1,2-dichloroethane and 1,2-dibromoethane. Substitution of Phe172 by 16 different amino acids provided four mutants with high activity (Phe172Trp, Phe172Tyr, Phe172His, and Phe172Met) and many other protein variants with detectable activity. These results support our proposal that this residue is important, but not essential for the catalysis of DhlA. Trp207 of LinB and Phe205 of DhaA interact with halide ion by their main chain atoms. This interaction cannot be easily probed by site-directed mutagenesis and would also be difficult to analyze by quantum mechanic calculations conducted with small model of the active site. Interaction strictly depends on position of the halide ion inside the active site cavity. Pro223 of DhlA is conserved in LinB (Pro208), DhaA (Pro206), and many other haloalkane dehalogenases with known primary structures (*40*). This residue lies at the bottom of the active site and its substitution by an amino acid with larger side chain would prevent efficient binding of the halogen atom between two primary halide-stabilizing residues. Val226 of DhlA, Ile211 of LinB, and Ile209 in DhaA stabilize halide ion by their side chains. Val226Gly, Val226Ala, and Val226Leu of DhlA were constructed and characterized by Schanstra et al. (*55*). Observed differences in catalytic rates of the mutant proteins were attributed to interaction of Val226 with the above-discussed Trp125 and Phe172. On the basis of current study, we propose that changes in the catalytic rates could also be related to intrinsic properties of the side chain of residue introduced to position 226 and its interaction with the halogen/halide. The residues Ile211 in LinB and Ile209 of DhaA are suitable targets for future mutagenesis experiments.

ACKNOWLEDGMENT

Petr Kulhánek (Masaryk University, Czech Republic) is greatly acknowledged for valuable advises on ab initio calculations. Aaron Oakley (University of Western Australia, Australia) is acknowledged for providing the high-resolution structure of LinB before its publication and Usman A. Chaudry (University of Manchester, Great Britain) is ac-

knowledged for linguistic revision of the manuscript. Academic Supercomputer Centre in Czech Republic is acknowledged for computational resources.

REFERENCES

1. Franken, S. M., Rozeboom, H. J., Kalk, K. H., and Dijkstra, B. W. (1991) *EMBO J. 10*, 1297−1302.
2. Newman, J., Peat, T. S., Richard, R., Kan, L., Swanson, P. E., Affholter, J. A., Holmes, I. H., Schindler, J. F., Unkefer, C. J., and Terwilliger, T. C. (1999) *Biochemistry 38*, 16105−16114.
3. Marek, J., Vevodova, J., Kuta-Smatanova, I., Nagata, Y., Svensson, L. A., Newman, J., Takagi, M., and Damborsky, J. (2000) *Biochemistry 39*, 14082−14086.
4. Ollis, D. L., Cheah, E., Cygler, M., Dijkstra, B., Frolow, F., Franken, S. M., Harel, M., Remington, S. J., Silman, I., Schrag, J., Sussman, J. L., Verschueren, K. H. G., and Goldman, A. (1992) *Proteing Eng. 5*, 197−211.
5. Nardini, M., and Dijkstra, B. W. (1999) *Curr. Opin. Struct. Biol. 9*, 732−737.
6. Russell, R. B., and Sternberg, M. J. E. (1997) *Protein Eng. 10*, 333−338.
7. Verschueren, K. H. G., Seljee, F., Rozeboom, H. J., Kalk, K. H., and Dijkstra, B. W. (1993) *Nature 363*, 693−698.
8. Damborsky, J., and Koca, J. (1999) *Protein Eng. 12*, 989−998.
9. Pries, F., Kingma, J., and Janssen, D. B. (1995) *FEBS Lett. 358*, 171−174.
10. Pries, F., Kingma, J., Krooshof, G. H., Jeronimus-Stratingh, C. M., Bruins, A. P., and Janssen, D. B. (1995) *J. Biol. Chem. 270*, 10405−10411.
11. Hynkova, K., Nagata, Y., Takagi, M., and Damborsky, J. (1999) *FEBS Lett. 446*, 177−181.
12. Verschueren, K. H. G., Kingma, J., Rozeboom, H. J., Kalk, K. H., Janssen, D. B., and Dijkstra, B. W. (1993) *Biochemistry 32*, 9031−9037.
13. Kennes, C., Pries, F., Krooshof, G. H., Bokma, E., Kingma, J., and Janssen, D. B. (1995) *Eur. J. Biochem. 228*, 403−407.
14. Krooshof, G. H., Ridder, I. S., Tepper, A. W. J. W., Vos, G. J., Rozeboom, H. J., Kalk, K. H., Dijkstra, B. W., and Janssen, D. B. (1998) *Biochemistry 37*, 15013−15023.
15. Schindler, J. F., Naranjo, P. A., Honaberger, D. A., Chang, C.-H., Brainard, J. R., Vanderberg, L. A., and Unkefer, C. J. (1999) *Biochemistry 38*, 5772−5778.
16. Damborsky, J., Kuty, M., Nemec, M., and Koca, J. (1997) *J. Chem. Inf. Comput. Sci. 37*, 562−568.
17. Verschueren, K. H. G., Franken, S. M., Rozeboom, H. J., Kalk, K. H., and Dijkstra, B. W. (1993) *J. Mol. Biol. 232*, 856−872.
18. Morris, G. M., Goodsell, D. S., Halliday, R. S., Huey, R., Hart, W. E., Belew, R. K., and Olson, A. J. (1998) *J. Comput. Chem. 19*, 1639−1662.
19. Bosma, T., Damborsky, J., Stucki, G., and Janssen, D. B. (2002) *Appl. Environ. Microbiol. 68*, 3582−3587.
20. Vriend, G. (1990) *J. Mol. Graphics 8*, 52−56.
21. Sali, A., and Blundell, T. L. (1993) *J. Mol. Biol. 234*, 779−815.
22. Damborsky, J., Bohac, M., Prokop, M., Kuty, M., and Koca, J. (1998) *Protein Eng. 11*, 901−907.
23. Stewart, J. J. P. (1990) *J. Comput.-Aided Mol. Des. 4*, 1−45.
24. Stewart, J. J. P. (1996) *Int. J. Quantum Chem. 58*, 133−146.
25. Cernohorsky, M., Kuty, M., and Koca, J. (1996) *Comput. Chem. 21*, 35−44.
26. Lightstone, F. C., Zheng, Y.-J., Maulitz, A. H., and Bruice, T. C. (1997) *Proc. Natl. Acad. Sci. U.S.A. 94*, 8417−8420.
27. Prokop, M., Damborsky, J., and Koca, J. (2000) *Bioinformatics 16*, 845−846.
28. Damborsky, J., Prokop, M., and Koca, J. (2001) *Trends Biochem. Sci. 26*, 71−73.
29. Ridder, I. S., Rozeboom, H. J., and Dijkstra, B. W. (1999) *Biol. Crystallogr. 55*, 1273−1290.
30. Frisch, M. J., Frisch, A., and Foresman, J. B. (1998) *Gaussian 98*, Gaussian, Inc., Pittsburgh, PA.
31. Nagata, Y., Hynkova, K., Damborsky, J., and Takagi, M. (1999) *Protein Expression Purif. 17*, 299−304.
32. Verschueren, K. H. G., Franken, S. M., Rozeboom, H. J., Kalk, K. H., and Dijkstra, B. W. (1993) *FEBS Lett. 323*, 267−270.
33. Schanstra, J. P., Ridder, I. S., Heimeriks, G. J., Rink, R., Poelarends, G. J., Kalk, K. H., Dijkstra, B. W., and Janssen, D. B. (1996) *Biochemistry 35*, 13186−13195.
34. Pikkemaat, M. G., Ridder, I. S., Rozeboom, H. J., Kalk, K. H., Dijkstra, B. W., and Janssen, D. B. (1999) *Biochemistry 38*, 12052−12061.
35. Maulitz, A. H., Lightstone, F. C., Zheng, Y. J., and Bruice, T. C. (1997) *Proc. Natl. Acad. Sci. U.S.A. 94*, 6591−6595.
36. Kuty, M., Damborsky, J., Prokop, M., and Koca, J. (1998) *J. Chem. Inf. Comput. Sci. 38*, 736−741.
37. Damborsky, J. (1998) *Protein Eng. 11*, 21−30.
38. Lightstone, F. C., Zheng, Y. J., and Bruice, T. C. (1998) *J. Am. Chem. Soc. 120*, 5611−5621.
39. Shurki, A., Strajbl, M., Villa, J., and Warshel, A. (2002) *J. Am. Chem. Soc. 124*, 4097−4107.
40. Jesenska, A., Bartos, M., Czernekova, V., Rychlik, I., Pavlik, I., and Damborsky, J. (2002) *Appl. Environ. Microbiol. 68*, 3724−3730.
41. Schanstra, J. P., Kingma, J., and Janssen, D. B. (1996) *J. Biol. Chem. 271*, 14747−14753.
42. Stucki, G., and Thuer, M. (1995) *Environ. Sci. Technol. 29*, 2339−2345.
43. Swanson, P. E. (1999) *Curr. Opin. Biotechnol. 10*, 365−369.
44. Holloway, P., Knoke, K. L., Trevors, J. T., and Lee, H. *Biotechnol. Bioeng. 59*, 520−523.
45. Marvanova, S., Nagata, Y., Wimmerova, M., Sykorova, J., Hynkova, K., and Damborsky, J. (2001) *J. Microbiol. Methods 44*, 149−157.
46. Gray, K. A., Richardson, T. H., Kretz, K., Short, J. M., Bartnek, F., Knowles, R., Kan, L., Swanson, P. E., and Robertson, D. E. (2001) *Adv. Synth. Catal. 343*, 607−617.
47. Pikkemaat, M. G., and Janssen, D. B. (2002) *Nucleic Acid Res. 30*, e35−5.
48. Krooshof, G. H., Kwant, E. M., Damborsky, J., Koca, J., and Janssen, D. B. (1997) *Biochemistry 36*, 9571−9580.
49. Otyepka, M., and Damborsky, J. (2002) *Protein Sci. 11*, 1206−1217.
50. Pries, F., Van den Wijngaard, A. J., Bos, R., Pentenga, M., and Janssen, D. B. (1994) *J. Biol. Chem. 269*, 17490−17494.
51. Schanstra, J. P., and Janssen, D. B. (1996) *Biochemistry 35*, 5624−5632.
52. Arnold, G. E., and Ornstein, R. L. (1997) in *Biomacromolecules: From 3-D to Applications* (Ornstein, R. L., Ed.) pp 215−229, Battelle Press, Columbus, OH.
53. Oakley, A. J., Prokop, Z., Bohac, M., Kmunicek, J., Jedlicka, T., Monincova, M., Kuta-Smatanova, I., Nagata, Y., Damborsky, J., and Wilce, M. C. J. (2002) *Biochemistry 41*, 4847−4855.
54. Damborsky, J. (1997) *Quant. Struct.-Act. Relat. 16*, 126−135.
55. Schanstra, J. P., Ridder, A., Kingma, J., and Janssen, D. B. (1997) *Protein Eng. 10*, 53−61.

BI026427V